Molecular Biology of the Cell
Vol. 15, 5408–5419, December 2004

Differential Contribution of Skeletal and Cardiac II-III Loop Sequences to the Assembly of Dihydropyridine-Receptor Arrays in Skeletal Muscle[D]

Hiroaki Takekura,*†‡ Cecilia Paolini,*†§ Clara Franzini-Armstrong,† Gerlinde Kugler,‖¶ Manfred Grabner,‖ and Bernhard E. Flucher¶#

†Department of Cell and Developmental Biology, University of Pennsylvania, Philadelphia, PA 19104; and ‖Departments of Medical Genetics, Molecular and Clinical Pharmacology and ¶Physiology and Medical Physics, Innsbruck Medical University, A-6020 Innsbruck, Austria

Submitted May 19, 2004; Accepted September 8, 2004
Monitoring Editor: Daniel Goodenough

The plasmalemmal dihydropyridine receptor (DHPR) is the voltage sensor in skeletal muscle excitation-contraction (e-c) coupling. It activates calcium release from the sarcoplasmic reticulum via protein–protein interactions with the ryanodine receptor (RyR). To enable this interaction, DHPRs are arranged in arrays of tetrads opposite RyRs. In the DHPR α_{1S} subunit, the cytoplasmic loop connecting repeats II and III is a major determinant of skeletal-type e-c coupling. Whether the essential II-III loop sequence (L720-L764) also determines the skeletal-specific arrangement of DHPRs was examined in dysgenic (α_{1S}-null) myotubes reconstituted with distinct α_1 subunit isoforms and II-III loop chimeras. Parallel immunofluorescence and freeze-fracture analysis showed that α_{1S} and chimeras containing L720-L764, all of which restored skeletal-type e-c coupling, displayed the skeletal arrangement of DHPRs in arrays of tetrads. Conversely, α_{1C} and those chimeras with a cardiac II-III loop and cardiac e-c coupling properties were targeted into junctional membranes but failed to form tetrads. However, an α_{1S}-based chimera with the heterologous *Musca* II-III loop produced tetrads but did not reconstitute skeletal muscle e-c coupling. These findings suggest an inhibitory role in tetrad formation of the cardiac II-III loop and that the organization of DHPRs in tetrads vis-à-vis the RyR is necessary but not sufficient for skeletal-type e-c coupling.

INTRODUCTION

The series of molecular events linking surface membrane depolarization to calcium release from the intracellular stores of the sarcoplasmic reticulum (SR) and ultimately to contraction of the myofibrils is collectively called excitation-contraction (e-c) coupling. In skeletal muscle, an essential requirement for e-c coupling is an allosteric interaction between L-type calcium channels, called dihydropyridine receptors (DHPRs), and the SR calcium release channels, called ryanodine receptors (RyRs). This includes an orthograde signaling by which DHPRs control the functional state of RyRs and a retrograde interaction by which RyRs affect the conductance of DHPRs (Nakai *et al.*, 1996). The relative location of RyRs and DHPRs within the signaling complex of the T-tubule/SR junctions is obviously critical for this interaction. Targeting of the DHPR channels into sites where they can closely interact with RyRs, which is at triads or peripheral couplings, is essential for their interaction with RyRs. Heterologous calcium channel α_1 subunits (α_{1C}, α_{1D}, and α_{1A}) expressed in dysgenic myotubes cause a restoration of e-c coupling (albeit dependent on extracellular calcium) only if they are endowed with an appropriate triad-targeting signal that causes them to cluster at triads (Flucher *et al.*, 2000a; Kasielke *et al.*, 2003). Moreover, two-domain fragments of the skeletal calcium channel α_{1S} subunit restore e-c coupling in the α_{1S} null-mutant myotubes only if expressed in a combination that results in their appropriate targeting to the triads (Ahern *et al.*, 2001; Flucher *et al.*, 2002). Thus, for e-c coupling the specific location of the channel is just as important as its function as voltage sensor and/or calcium channel.

The allosteric DHPR–RyR interaction underlying skeletal muscle e-c coupling requires that the two proteins are associated through a link that allows a physical channel to channel conformational coupling. Structural comparison of DHPR–RyR association in skeletal and cardiac muscle has shown that in the former the two channels are arranged in highly ordered, congruent arrays so that groups of four DHPRs (constituting a tetrad) are located exactly opposite every other RyR homotetramer. Because cardiac muscle, in which the DHPR and RyR communicate via the soluble second messenger calcium, lacks the tetradic organization of

Article published online ahead of print. Mol. Biol. Cell 10.1091/mbc.E04–05–0414. Article and publication date are available at www.molbiolcell.org/cgi/doi/10.1091/mbc.E04–05–0414.

[D] The online version of this article contains supplemental material at MBC Online (http://www.molbiolcell.org).

* These two authors contributed equally to this work.

Present addresses: ‡Department of Physiological Sciences, National Institute of Fitness and Sports, Kanoya, Kagoshima, 891-2393, Japan; §Ce.S.I. Center for Research on Aging, Fondazione "G.d'Annunzio," Chieti, Italy.

Corresponding author. E-mail address: bernhard.e.flucher@uibk.ac.at.

Abbreviations used: DHPR, dihydropyridine receptor; e-c coupling, excitation-contraction coupling; GFP, green fluorescent protein; RyR1, type 1 ryanodine receptor; SR, sarcoplasmic reticulum; T-tubule, transversal tubule.

DHPRs, the tetrads in skeletal muscle were proposed to be the structural correlates of the allosteric coupling between the two channels (Sun *et al.*, 1995; Protasi *et al.*, 1996; Proenza *et al.*, 2002). This hypothesis is further supported by the observation that invertebrate skeletal muscles follow the cardiac pattern both structurally and functionally (Hencek and Zachar, 1977; Araque *et al.*, 1994; Gilly and Scheuer, 1994; Erxleben and Rathmayer, 1997; Takekura and Franzini-Armstrong, 2002). The skeletal/cardiac dichotomy (as well as that between vertebrate and invertebrate skeletal muscles) provides a useful paradigm for exploring the molecular and structural requirement for the bidirectional interaction in vertebrate skeletal muscles. Experiments using chimeras of skeletal (RyR1) and cardiac (RyR2) RyRs expressed in RyR knock-out myotubes have shown that bidirectional signaling is linked to the presence of congruent DHPR-RyR arrays (Protasi *et al.*, 2002). Extensive studies of α_1 subunit chimeras expressed in dysgenic (α_{1S} DHPR null-mutant) myotubes indicate that a sequence of 45 residues in the α_{1S} DHPR II-III loop (L720-L764) contain molecular determinants of critical importance for skeletal muscle e-c coupling as well as retrograde current enhancement (Tanabe *et al.*, 1990; Nakai *et al.*, 1998; Grabner *et al.*, 1999; Wilkens *et al.*, 2001; Kugler *et al.*, 2004a). Consequently these 45 α_{1S} residues may contain a site of a protein–protein interaction between the DHPR and the RyR1.

Here, we test the hypothesis that the specific organization of DHPRs into tetrads is a structural requirement for the skeletal muscle-specific link between the voltage sensor and the calcium release channel. Dysgenic myotubes were reconstituted with α_1 subunits and II-III loop chimeras with known e-c coupling properties and their structural organization was analyzed using parallel immunolabeling and freeze-fracture electron microscopy to detect targeting of the channel construct into the junctions and the formation of DHPR tetrads, respectively. Tetrads are present in all myotubes transfected with constructs that reconstitute skeletal type DHPR–RyR interactions, indicating the requirement of a specific positioning of the two molecules for the allosteric coupling. Interestingly, however, tetrads are also present in cells expressing one chimera that does not restore skeletal e-c coupling. Thus, the molecular determinants of the functional coupling are not necessarily the same as those required for a specific anchoring of the two proteins. This may involve domains of the α_{1S} other than the critical segment of the II-III loop and perhaps other subunits.

MATERIALS AND METHODS

Construction of DHPR α_1 Chimeras

The cDNA construction of the DHPR α_1 subunits and of the II-III loop chimeras as well as their insertion into the proprietary mammalian expression vector pGFP37 (Grabner *et al.*, 1998) 3′ in-frame to the coding region of a modified green fluorescent protein (GFP) was described to detail previously: GFP-α_{1S} and GFP-α_{1C} in Grabner *et al.* (1998); GFP-SkLC and GFP-SkLCS$_{46}$ in Grabner *et al.* (1999), and GFP-SkLM and GFP-SkLMS$_{45}$ in Wilkens *et al.* (2001).

Newly constructed chimeras containing of sequences of the rabbit skeletal muscle DHPR α_{1S} (Sk; Tanabe *et al.*, 1987), the rabbit cardiac DHPR α_{1C} (C; Mikami *et al.*, 1989), and the α_1 subunit from house fly (*Musca domestica*) body wall muscle (M; Grabner *et al.*, 1994) are briefly described below (nucleotide numbers [nt] are given in parentheses).

GFP-CSk3: The *Bam*HI-*Eco*RV fragment (nt 1265–4351; α_{1C}-numbering) of clone CSk3 (Tanabe *et al.*, 1990), containing the cDNA coding for the skeletal II-III loop, was ligated into the corresponding restriction enzyme (RE) sites of clone GFP-α_{1C} (Grabner *et al.*, 1998).

GFP-CLM: Fusion-PCR was used to combine α_{1C} sequence with the *Musca* II-III loop cDNA (nt 1993–2370). The upstream α_{1C} fragment created a C/M transition site (C2349/M1993) and included the cardiac *Eco*RI RE site (nt 2215). The downstream α_{1C} fragment created an M/C transition site (nt M2370/C2790) and carried the cardiac *Apa*I RE site (nt 3491). PCR fusion products were used to isolate an *Eco*RI-*Nde*I fragment (nt C2215-M2294) and a *Nde*I-*Apa*I fragment (nt M2294-C3491). Both fragments were coligated into the corresponding *Eco*RI/*Apa*I polylinker RE sites of pBluescript (Stratagene, La Jolla, CA) to yield a subclone. Subsequently, a *Bam*HI-*Eco*RI fragment of α_{1C} cDNA (nt 1265–2215) was ligated into the corresponding polylinker RE sites of the subclone. Finally the *Bam*HI-*Apa*I (nt 1265–3491) insert of the subclone was coligated with an *Apa*I-*Eco*RV fragment of α_{1C} (nt 3491–4351) into the corresponding RE sites (nt 1265/4351) of GFP-α_{1C} (Grabner *et al.*, 1998). Preparative polymerase chain reaction (PCR) was performed by using proofreading *Pfu Turbo* DNA polymerase (Stratagene). The integrity of all cDNA sequences generated and modified by PCR was confirmed by sequence analysis (MWG Biotech, Ebersberg, Germany).

Transfection

The DHPR cDNAs were expressed in myotubes derived from the dysgenic cell line GLT (Powell *et al.*, 1996). cDNA encoding the α subunit of the human surface antigen CD8 (Jurman *et al.*, 1994) was cotransfected to enable a subsequent identification of expressing myotubes by polystyrene beads coated with CD8 antibodies (Dynal, Hamburg, Germany). GLT cells were plated on carbon-coated class coverslips and on Thermanox coverslips (Nalge Nunc, Napperville, IL). At the onset of myoblast fusion (2 d after addition of differentiation medium), the cultures were transfected using the liposomal transfection reagent FuGene according to the manufacture's protocol (Roche Diagnostics, Mannheim, Germany).

Immunofluorescence Labeling

Four days after transfection, the cultures growing on glass were fixed with 100% methanol at −10°C for double immunolabeling with a monoclonal anti-GFP antibody at 1:4000 (Molecular Probes, Eugene, OR) and the affinity-purified antibody no.162 against the RyR1 at a dilution of 1:5000 (Giannini *et al.*, 1995), as described by Flucher *et al.* (1994). An Alexa-488–conjugated goat anti-mouse antibody was used with anti-GFP so that the antibody label and the intrinsic GFP signal were both recorded in the green channel. Alexa-594–conjugated goat anti-rabbit was used to detect anti-RyR1 to achieve a wide separation of the excitation and emission bands in the double-labeling experiments. Controls, for example, the omission of primary antibodies and incubation with inappropriate antibodies, were routinely performed. Images were recorded on a Zeiss Axiophot microscope by using a cooled charge-coupled device camera and METAVIEW image-processing software (Universal Imaging, West Chester, PA). All experiments were repeated several times, and only those experiments that showed a high efficiency of transfection (fraction of GFP-positive myotubes) and a high degree of differentiation (coclustered distribution of DHPR construct and RyR1) of the myotubes were chosen for freeze-fracture analysis.

Freeze-Fracture

Cultures on Thermanox were rinsed in phosphate-buffered saline (PBS), incubated with a 0.25% suspension of CD-8 beads for 10 min, rinsed again gently in PBS and fixed with 3.5% glutaraldehyde in 0.1 M neutral cacodylate buffer at neutral pH (both from Sigma-Aldrich, St. Louis, MO) at room temperature. Samples were stored in glutaraldehyde at 4°C until processing for freeze-fracture. Small pieces of the coverslips containing myotubes labeled by CD8 beads were cut out and infiltrated with 30% glycerol. The coverslip was mounted with the cells facing a droplet of 30% glycerol, 20% polyvinyl alcohol on a gold holder, and then frozen in liquid nitrogen-cooled propane (Cohen and Pumplin, 1979; Osame *et al.*, 1981). The coverslip was flipped off to produce a fracture that followed the culture surface originally facing the coverslip. The fractured surfaces were shadowed with platinum unidirectionally at 45° and then replicated with carbon in a freeze-fracture apparatus (model BFA 400; Balzers, Milan, Italy). Sections and replicas were photographed in a 410 Electron Microscope (Philips Electron Optics, Mahwah, NJ).

Quantitation of Particle Parameters

Association of particles with orthogonal arrays corresponding to RyR1 arrays and frequency of three- and four-particle tetrads were assessed as described in Protasi *et al.* (2000). Briefly, we first selected clusters that were most highly populated with particles and/or tetrads and further limited the measurements within a cluster to areas that had coherent arrays with the same orientation. For areas that show tetrads, dots were placed in the centers of a few most obvious tetrads, and the dot array was then extended into the adjacent areas, maintaining the same spacing. For particle clusters that did not show tetrads or any apparent order, a comparable array of dots with the appropriate spacing was superimposed on the image. Each particle within the dotted region was then classified as either belonging to the array (if clustered around the dots), or having a random disposition (if located at some distance from the dots). Furthermore, the number of particles constituting three- and four-particle tetrads was counted separately in each array and related to the total number of particles in the array.

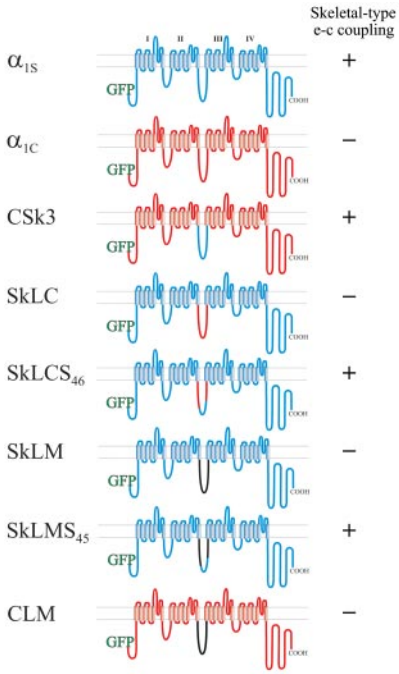

Figure 1. Transmembrane models of skeletal and cardiac DHPR α_1 subunits and of skeletal/cardiac and *Musca* II-III loop chimeras. DHPR constructs were N-terminally fused to GFP. Rabbit skeletal muscle α_{1S} sequence is indicated in blue, rabbit cardiac α_{1C} sequence in red, and *M. domestica* α_1 sequence in black; I–IV, homologous repeats of α_1 subunits. The ability of the chimeras to restore skeletal-type e-c coupling properties is indicated at the right of the schemes.

RESULTS

DHPR Constructs with Distinct e-c Coupling Properties

To test whether the α_{1S} II-III loop sequence, which is critical for skeletal muscle e-c coupling, also determines the skeletal-specific organization of DHPRs in tetrads, we expressed GFP fusion proteins of skeletal and cardiac α_1 subunits and chimeras thereof in dysgenic (α_{1S}-null) myotubes. Figure 1 shows all constructs used in the present study and indicates their known e-c coupling properties, as they were determined in previous work (Tanabe *et al.*, 1990; Nakai *et al.*, 1998; Grabner *et al.*, 1999; Wilkens *et al.*, 2001) or, in the case of CLM, in the present study (see Supplemental Figure 1). The constructs fall into three groups: the wild-type skeletal and cardiac channel isoforms, α_{1S} and α_{1C}; pure skeletal/cardiac II-III loop chimeras (CSk3, SkLC, and $SkLCS_{46}$); and chimeras, in which the II-III loop was replaced for the structurally dissimilar II-III loop of the house fly channel (SkLM, $SkLMS_{45}$, and CLM). Previous studies in which these constructs or their non-GFP–tagged versions were expressed and analyzed in dysgenic myotubes showed that all those channel isoforms and chimeras containing either the entire skeletal II-III loop (α_{1S}, CSk3) or a critical portion (residues L720 to L764) of it ($SkLCS_{46}$ and $SkLMS_{45}$), show calcium-independent e-c coupling as well as current amplification, representing the characteristic features of skeletal-type orthograde and retrograde coupling of the DHPR and RyR1 (Tanabe *et al.*, 1990; Nakai *et al.*, 1998; Grabner *et al.*, 1999; Wilkens *et al.*, 2001; Kugler *et al.*, 2004a).

Localization of DHPR Constructs in Plasma Membrane/SR and T-Tubule/SR Junctions

The proper targeting and incorporation of the recombinant α_1 subunits into junctions opposite to the RyR1 is a precondition for studying their potential in restoring e-c coupling or their distinct arrangement relative to the junctional RyR1 arrays. We used double immunofluorescence labeling of the GFP-tagged α_1 subunits and chimeras to demonstrate the correct localization in junctions with the SR. The use of anti-GFP to label the GFP-α_1 subunit fusion proteins permitted us to localize all constructs with the same antibody. A specific α_{1S} antibody gave the same results for those constructs containing the antibody epitope (Kugler *et al.*, 2004b). Anti-GFP labeling showed that approximately one-third of the dysgenic myotubes expressed the α_1 subunit constructs. Figure 2 shows the clustered distribution pattern observed with all tested α_1 subunit constructs in the majority of the myotubes. This clustered distribution pattern is typical for triad proteins in skeletal myotubes (Flucher *et al.*, 1994). In a minor subpopulation of either poorly differentiated or heavily overexpressing myotubes, the DHPRs remained diffusely located in the ER/SR (Flucher *et al.*, 2000b). Overall, no differences in expression and distribution detectable by immunocytochemistry were observed with the different constructs used in this study. Most importantly, α_1 subunits known to express skeletal e-c coupling properties (α_{1S}, CSk3, $SkLCS_{46}$, and $SkLMS_{45}$) and those with nonskeletal properties (α_{1C}, SkLC, SkLM, and CLM) showed the same clustered distribution pattern.

The DHPR clusters showed a high degree of colocalization with the clusters of RyR1 (Figure 2, examples indicated by arrows). A colocalization of DHPR clusters in the plasma membrane or T-tubules with RyR1 clusters of similar size and shape in the sarcoplasmic reticulum (SR) is indicative of a localization of both proteins in junctions between these membrane systems (Flucher *et al.*, 1994). In cultured myotubes in general and in dysgenic myotubes of the GLT cell line in particular, the majority of these junctions are localized in the periphery of the cells, both on the dorsal and ventral side. Thus, these coclusters represent either peripheral junctions between the plasma membrane and the SR or junctions between shallow T-tubules and the SR. Considering the transfection efficiency, the expression patterns, and the subcellular distribution of the recombinant α_1 subunits, it was to be expected that they can be observed in freeze-fractures through the ventral plasma membrane of a subset of myotubes in the transfected cultures.

Freeze-Fracture Analysis Reveals the Distinct Arrangement of Skeletal and Cardiac DHPRs

Under the conditions used, the fracture plane follows almost exclusively the plasmalemma on the side of the cells facing the coverslip. The cytoplasmic leaflet of the membrane is replicated, whereas the outer leaflet is discarded. The replicated cytoplasmic surfaces from most of the cells in all cultures used had the structural characteristic of nontransfected dysgenic myotubes: a random distribution of intramembranous particles of variable size, with no indication of clustering (see Figure 2, C and D, in Takekura *et al.*, 1994). This was not unexpected considering the transfection efficiency and the degree of differentiation observed in fluorescence microscopy (see above). A small percentage of myotubes, however, displayed numerous small patches of membrane that were occupied by clusters of large particles with a fairly uniform size (Figures 3–6). The patches were scattered over either the whole cell surface or a portion of it

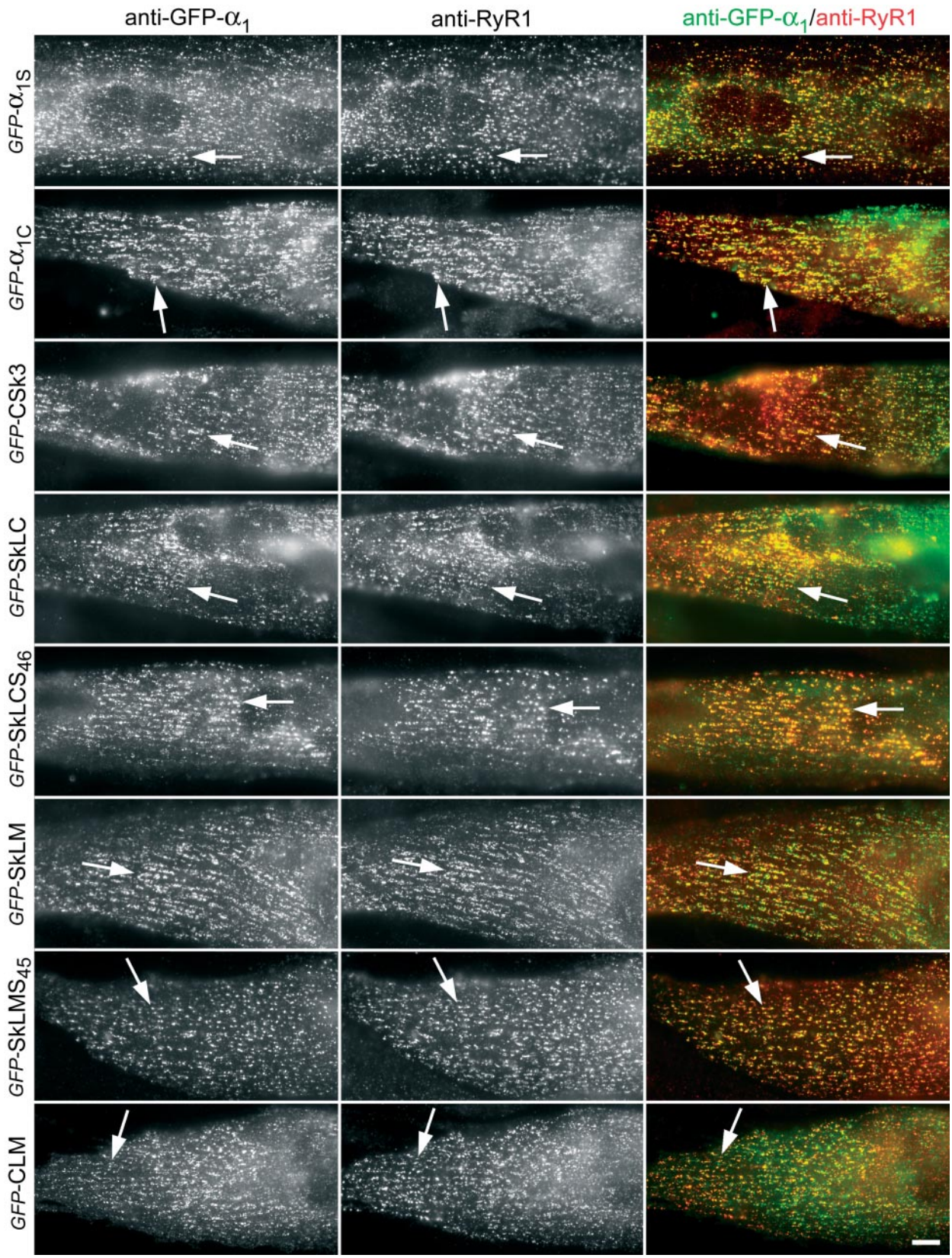

Figure 2. Immunolocalization of the GFP-α_1 subunit constructs in calcium release units of reconstituted dysgenic myotubes. GLT myotubes were transfected with a range of GFP-tagged α_1 subunit isoforms and chimeras. Double immunofluorescence labeling with anti-GFP (left column) and anti-RyR1 (middle column) shows that all α_1 subunits and chimeras are located in clusters that are colocalized with RyR1 clusters (examples indicated by arrows). Colocalization of α_1 subunit clusters and RyR1 clusters is indicative of their localization in T-tubule/SR and plasma membrane/SR junctions. In the merged color image (right column) colocalization of anti-GFP stain (green) and anti-RyR1 stain (red) results in yellow clusters. Bar, 10 μm.

Table 1. Particle and tetrad sizes

Construct	Particle size (nm)	Tetrad spacing (nm)
α_{1S}	8.2±1.2	42.7±3.1
α_{1C}	10.5±1.6	
CSk3	10.2±1.8	42.9±3.7
SkLC	10.0±1.4	
$SkLCS_{46}$	7.9±1.2	44.6±3.6
SkLM	8.3±1.0	44.0±4.8
$SkLMS_{45}$	8.7±1.2	42.8±4.2
CLM	10.0±1.6	

Mean ± SD; number of measurements: particle size, n = 60; tetrad spacing, n = 48–50.

and often, but not always, had a slightly domed shape. The domed shape is characteristic of the sites where SR cisternae, decorated by feet, push up against the plasmalemma. The overall size and distribution of these patches was consistent with the clusters observed in fluorescence microscopy. The size of the large particles within the clusters, measured at right angle to the direction of shadow, is ~8 nm for the skeletal DHPR-based constructs (with one exception) and ~10 nm for the cardiac DHPR-based chimeras and SkLC (Table 1). The particles within these patches were identified as DHPRs based on the following observations: 1) their presence in a minority of cells in the transfected cultures; 2) their size (compare with Franzini-Armstrong, 1984; Franzini-Armstrong and Kish, 1995; Takekura *et al.*, 1995; Protasi *et al.*, 1997, 1998, 2000); 3) their location over domed membrane patches (as expected by the localization of RyRs and DHPRs seen by immunolabeling); and 4) their arrangement into tetrads where applicable (see below).

Figure 3 illustrates the characteristic skeletal and cardiac arrangement of the large integral membrane particles in dysgenic myotubes expressing α_{1S} and α_{1C}, respectively. In cells transfected with α_{1S} (Figure 3, A–D), the particles were arranged in arrays of tetrads, located on slightly domed membrane patches, as first shown by Takekura *et al.* (1994). The membrane particles marked the corners of virtual squares (tetrads), and the tetrads were themselves regularly arranged into larger orthogonal arrays. This is indicated for each cluster in Figures 3–5 by showing the original image on the left (e.g., Figure 3, A and C) and a "dotted" copy of the same image on the right (e.g., Figure 3, B and D). The dots define an orthogonal array, and at each dot position one can detect up to four particles delineating the corners of squares. Thus, α_{1S} is arranged in tetrads and particles between the tetrads within an array are rarely found, but the tetrads are not always complete. The average intertetrad spacing of 42.7 nm (Table 1) is similar to values measured in wild-type mouse muscle in vivo, and it indicates an association of tetrads with alternate feet within the RyR array (Takekura *et al.*, 1994; Franzini-Armstrong and Kish, 1995).

The corresponding membrane particles in cultures transfected with α_{1C} also were detected in clusters located on membrane patches that are often slightly domed (Figure 3E). This indicates the apposition of the DHPR clusters to SR cisternae and is consistent with the colocalization of α_{1C} and the RyR1 shown by immunolabeling (Figure 2). However, the clusters of the cardiac DHPR isoforms had a loose arrangement of particles, with variable interparticle distances and no indication of tetrads or any other regular order (Figure 3, E and F). The lack of tetrad formation by α_{1C} is not due to a low density of the DHPRs within junctional patches. Column 6 in Table 2 shows that the density of particles in the analyzed regions within junctional patches of α_{1C}-transfected cells is only slightly lower than the density of particles in tetrad-containing regions of α_{1S}-expressing cells. By contrast to the loose particle arrangement of α_{1C}, all clusters in the α_{1S}-expressing cells contained some tetrads.

Skeletal/Cardiac DHPR α_1 Subunit Chimeras Indicate a Role of the II-III Loop in Tetrad Formation

Because a sequence in the skeletal DHPR α_1 II-III loop had been shown to confer skeletal e-c coupling properties onto the cardiac channel isoforms, II-III loop chimeras were tested for their ability to restore tetrad formation in dysgenic myotubes. CSk3, a cardiac channel α_1 subunit with the entire II-III loop from the skeletal α_{1S}, restored arrays of tetrads (Figure 4, A–D). Conversely, SkLC, which is the skeletal channel with the entire II-III loop from cardiac α_{1C}, totally failed to restore tetrads, or any other order in the disposition of the particles (Figure 4E). The ability to form arrays of tetrads was restored to this chimera when the skeletal sequence L720-Q765 was reinserted into the corresponding

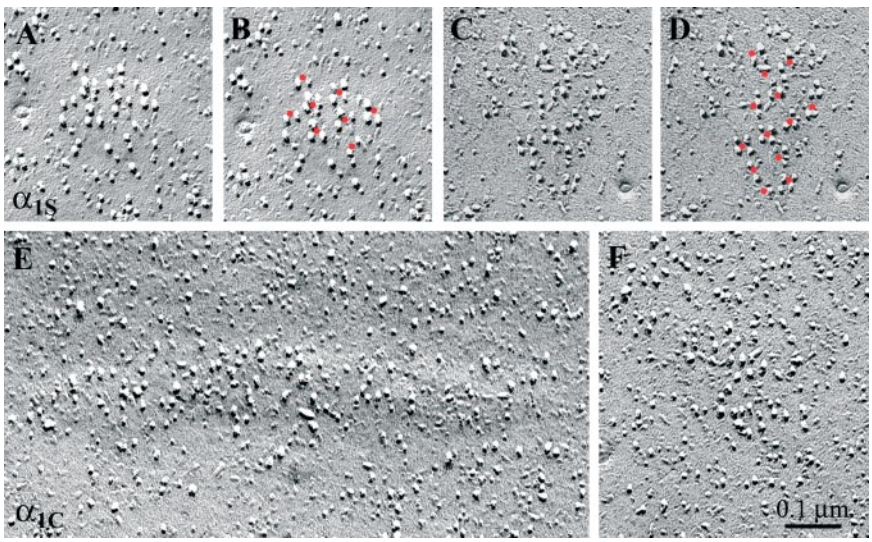

Figure 3. Restoration of DHPR tetrads by α_{1S} but not by α_{1C}. Freeze-fracture replicas of dysgenic myotubes reconstituted either with GFP-α_{1S} (A–D) or GFP-α_{1C} (E and F) showing the cytoplasmic leaflet of the plasmalemma. In the α_{1S} expressing cells, small, slightly domed membrane patches are occupied by large integral membrane particles forming groups of up to four particles. These tetrads are regularly arranged in orthogonal arrays (see tetrads marked with a red dot in the center in the duplicate images B and D). One to four particles are clustered around each dot and the membrane between the tetrads is clear of additional particles. α_{1C}-expressing cells also express clusters of large particles in domed membrane patches (E and F). However, these particles are not arranged in tetrads or orthogonal arrays.

Table 2. Particle statistics

Construct	% Particles associated/orthogonal array	% Particles in 3/4-particle tetrads	Ave. ratio of 4/3-particle tetrads	Ave. area of analyzed domains (μm^2)	Ave.particles/area (no./μm^2)
α_{1S}	92	77	1.27	0.0227	1075
α_{1C}	7	5	0	0.0235	802
CSk3	93	73	1.05	0.0236	948
SkLC	6	6	0.08	0.0222	1019
$SkLCS_{46}$	92	73	0.97	0.0241	950
SkLM	83	58	0.50	0.0188	947
$SkLMS_{45}$	97	88	1.43	0.0460	1017
CLM	6	4	0	0.0096	1675

region of the cardiac II-III loop ($SkLCS_{46}$) (Figures 4, F–I). Thus, in chimeras composed exclusively of α_{1S} and α_{1C} the origin of the II-III loop sequence L720-Q765 determined the ability to restore tetrads in dysgenic myotubes, and tetrad formation and skeletal e-c coupling properties went hand in hand.

This clear correlation of structure and function, however, failed when analyzing a chimera with a more heterologous II-III loop, SkLM, a construct similar to SkLC, but with the II-III loop derived from an insect α_1 subunit (*Musca domestica*). Unexpectedly, SkLM, which is unable to restore e-c coupling (Wilkens *et al.*, 2001), restored tetrads, although with reduced effectiveness (Table 2; see below). In this construct (Figure 5, A–D), tetrads were arranged in defined arrays, but they were not always complete. Furthermore, some additional particles not positioned at the corners of the tetrad array were present within the array, making it harder to detect, particularly when the array is not marked by the "dots." The additional particles intercalated within the SkLM arrays are smaller than the typical DHPR particles and thus they were not included in the counts of Table 2 (see below). Interestingly, reinsertion of the skeletal sequence L720-L764 into the *Musca* II-III loop of SkLM, to form $SkLMS_{45}$, resulted in a construct that formed tetrad arrays very well. Indeed, of all analyzed constructs this was the one that formed the most extensive and ordered arrays (Figure 5, E–I). Within the arrays, the tetrads were very complete and well ordered, and no particles other than those belonging to the array were observed (Figure 5, F–I).

To test whether the *Musca* II-III loop itself contains the tetrad-forming property, this loop was inserted into the cardiac channel creating chimera CLM. Functional analysis confirmed that this construct expressed calcium channels with cardiac current properties in dysgenic myotubes (see Supplemental Figure 1). Depolarization-induced calcium transients ceased upon application of cadmium/lanthanum, indicating that the calcium transients were dependent on influx of calcium through the L-type channel. Moreover, combined patch-clamp and calcium recordings with fluorescent indicators showed that α_{1C} and CLM had very similar calcium currents and cytoplasmic calcium transients. Thus, as expected, CLM restored cardiac e-c coupling in dysgenic myotubes. Freeze-fracture analysis of CLM-transfected cultures showed that CLM membrane particles assumed the cardiac disposition (Figure 6). Thus, the highly heterologous II-III loop sequence of the *Musca* channel could not confer tetradic organization to α_{1C} expressed in dysgenic myotubes.

Quantitative Analysis of the Tetrad-forming Potential of DHPR Constructs

In addition to detecting tetrads qualitatively, we quantitatively assessed the ability of various constructs to restore the skeletal type DHPR-RyR association by specific linking to the RyR array. To this end, we counted tetrad frequencies within defined DHPR clusters. Our aim was to define the ability of a given chimera to form tetrads under the best circumstances, rather than to estimate the average frequency of tetrads in each culture. Thus, we specifically selected clusters that seemed most populated by tetrads. Groups of particles were counted as tetrad-like configurations based on visual identification, taking into consideration that tetrads can get somewhat distorted during the fracturing procedure and that platinum deposit varies somewhat between replicas. Two sets of quantitative data were obtained. First, the occupancy by particles of sites associated with an orthogonal array of dots placed at intervals presumably marking the position of alternate feet. This indicates whether a given construct preferentially associates with the underlying RyR1 array or not. Second, the occurrence of complete tetrads within each array was assessed, which provides some information about the potential cooperativity of tetrad formation and the differentiation status of the array.

Table 2 shows that both the frequency of particles' association with arrays (column 1) and the occurrence of three- and four-particle tetrads (columns 2 and 3) are clearly separated into two categories: constructs with a high degree of organization and cooperativity (α_{1S}, CSk3, $SkLCS_{46}$, SkLM, and $SkLMS_{45}$) and those with a low degree of order (α_{1C}, SkLC, and CLM). In the ordered group, three- and four-particle tetrads account for a high percentage of the total particles (column 2). The ratio of four- to three-particle tetrads, which is indicative of how complete the arrays are, is highest in α_{1S} and $SkLMS_{45}$, and lower but still high in CSk3 and $SkLCS_{46}$ (column 3). In SkLM-expressing cells, tetrads are clearly present and are part of arrays, but they are less complete (columns 2 and 3). In the group with no evident order (α_{1C}, SkLC, CLM), a very small percentage of particles is apparently associated with arrays and were counted as tetrad-like structures, but these should be attributed to coincidental grouping. Columns 4 and 5 in Table 2 show that the clusters selected for counting were of similar size (with the exceptions of $SkLMS_{45}$ that had very large clusters and CLM that tended to have small clusters) and had similar densities of particles. The similarity in overall density of particles indicates that lack of tetrads for α_{1C}, SkLC, and CLM constructs is not due to a lack of available DHPRs. Although α_{1C} clusters had a slightly (~20%) lower particle density, the striking differences in the degree of order cannot

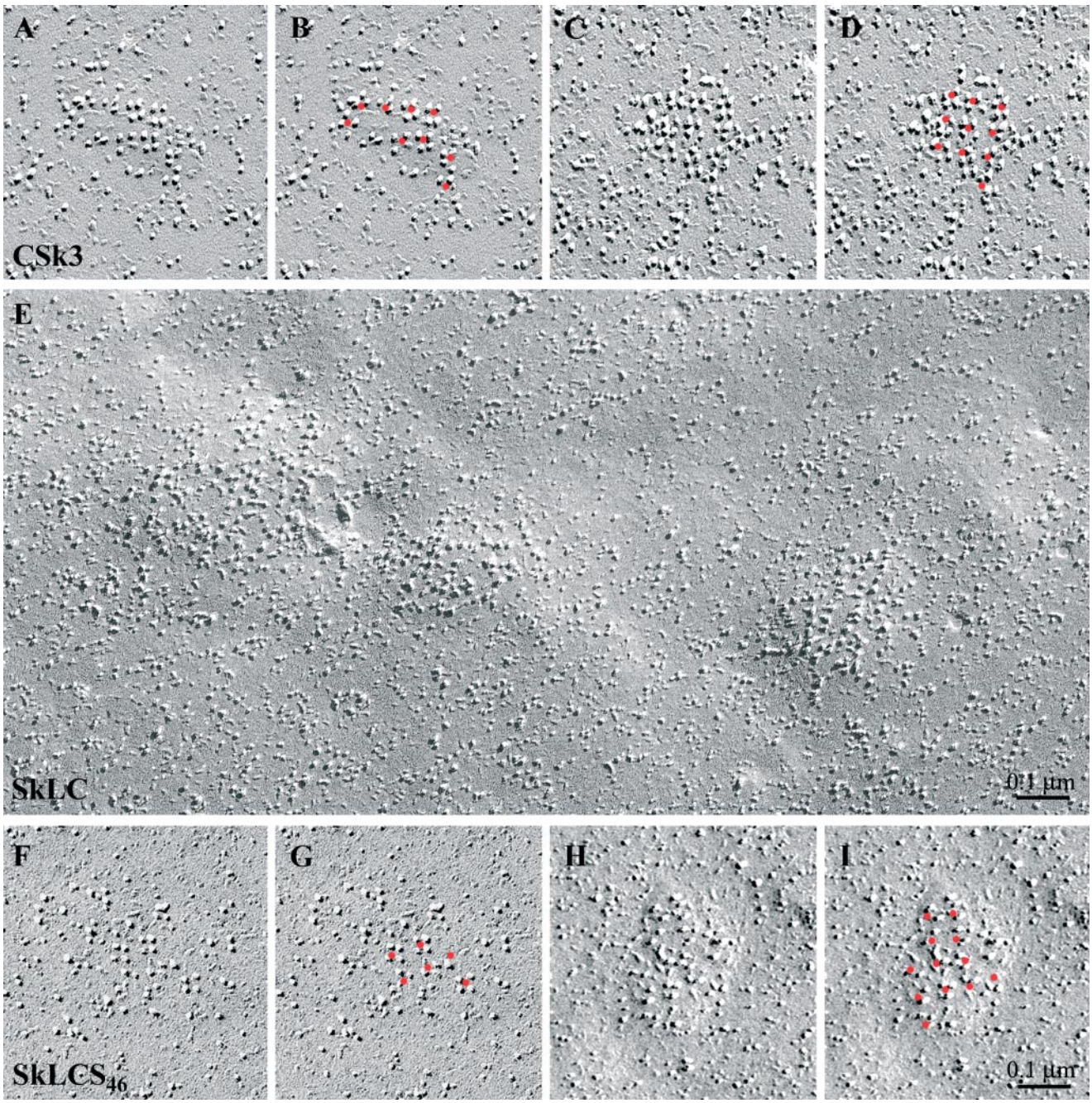

Figure 4. Skeletal II-III loop sequences confer the ability for tetrad formation to the cardiac DHPR. Freeze-fracture replicas of skeletal/cardiac II-III loop chimeras expressed in dysgenic myotubes. Tetrads (complete and incomplete) are marked with a red dot in duplicate images (B, D, G, and I) to indicate their arrangement in orthogonal arrays. CSk3, a cardiac DHPR containing the skeletal II-III loop restores tetrads (A–D), whereas SkLC, the mirror chimera with a cardiac II-III loop in a skeletal background does not (E). Reinsertion of the skeletal sequence L720-Q765 into SkLC (to form $SkLCS_{46}$) restores the ability to form tetrads (F–I).

be explained by differences in either cluster size or occupancy of the clusters by particles.

Together, the qualitative and quantitative analysis of the freeze-fracture preparations indicated that between skeletal and cardiac α_1 subunits and the II-III loop chimeras thereof the capacity to form tetrads correlated with skeletal or cardiac e-c coupling properties. But the ability of chimera SkLM to form tetrads indicated that tetrad formation might be necessary but certainly not sufficient for calcium-independent, skeletal muscle e-c coupling.

DISCUSSION

The direct coupling hypothesis for skeletal muscle e-c coupling was greatly inspired by the observations that the voltage sensors, the DHPRs, are regularly arranged in tetrads opposite the four corners of every other RyR1 homotetramer (Block *et al.*, 1988) and that the functional DHPR–RyR interaction is bidirectional (Nakai *et al.*, 1996). It is reasonable to expect that the precise relative positioning of the two molecules is a necessary requirement for functional coupling.

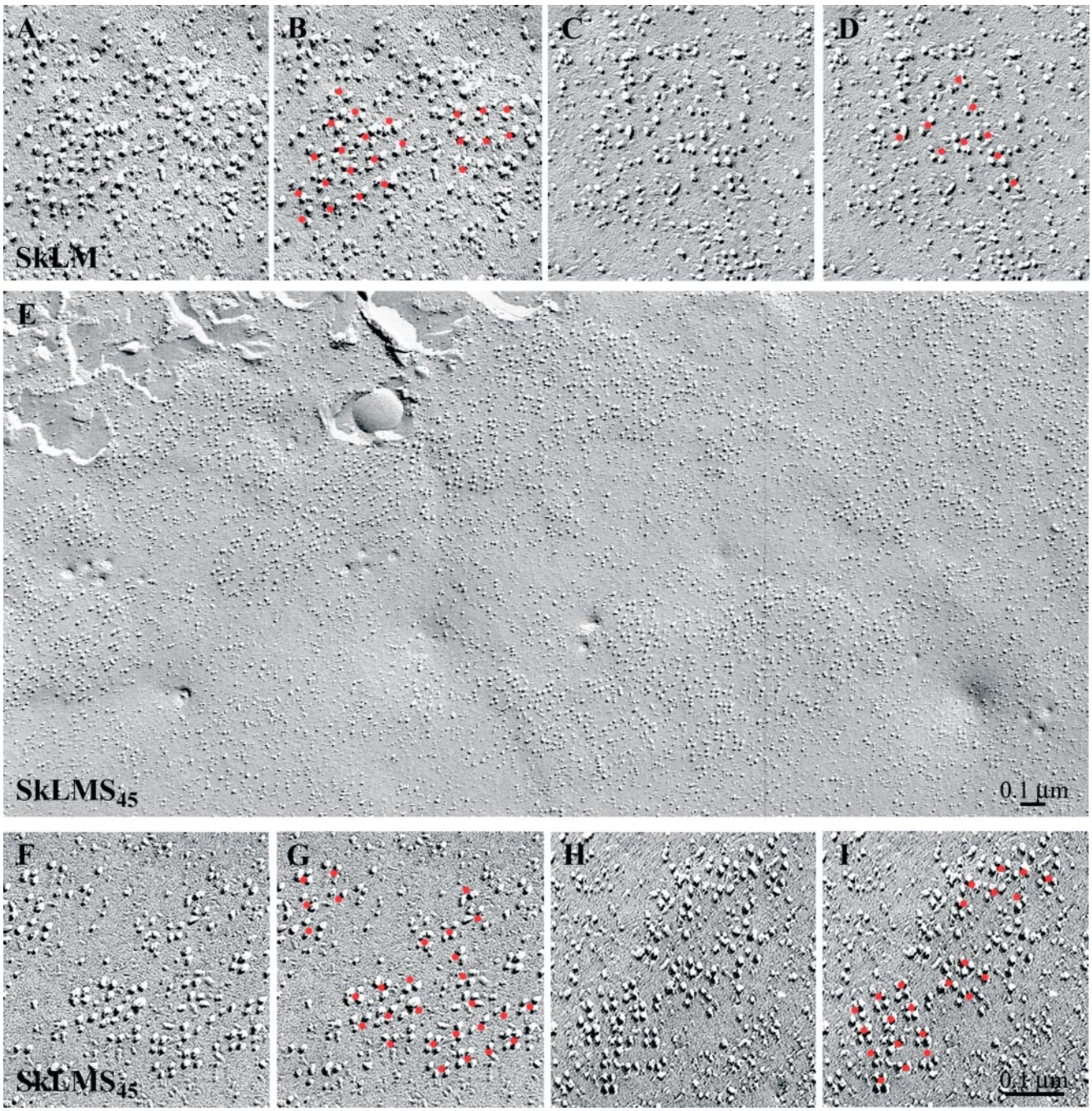

Figure 5. Replacing the α_{1S} II-III loop with the highly heterologous II-III loop of the *Musca* α_1 subunit does not abolish tetrad formation. Expression of chimera SkLM, a skeletal DHPR with the *Musca* II-III loop sequence, restores tetrad formation in dysgenic myotubes, although not as effectively as α_{1S} II-III loop constructs (A–D). The tetrads are less complete (see frequent occurrence of one- and two-particle "tetrads" around red dots in B and D), and particles that cannot clearly be associated to tetrads are sometimes seen within the arrays. Reinsertion of the skeletal sequence L720-L764 into SkLM (to form $SkLMS_{45}$) increases the ability to form tetrads, both with respect to completeness of tetrads (F–I) and to the size of the tetrad arrays (E).

With the characterization of molecular domains of the DHPR critically involved in the tissue-specific functional interaction with the RyR1 (Tanabe *et al.*, 1990; Nakai *et al.*, 1998; Grabner *et al.*, 1999; Wilkens *et al.*, 2001), the question arose whether the same sequences also are responsible for the structural organization of the DHPR opposite the RyR1. Considering exclusively the results obtained with the skeletal/cardiac II-III loop chimeras, our present findings, combined with the functional tests by Nakai *et al.* (1998) and Grabner *et al.* (1999) would suggest a simple model in which a 46-amino acid sequence in the skeletal II-III loop is of critical importance both for skeletal-type e-c coupling and for arranging the DHPR into tetrads. This would not preclude that other parts of the channel that are conserved between the two isoforms also may participate in DHPR–RyR1 interactions involved in tetrad formation and/or e-c coupling.

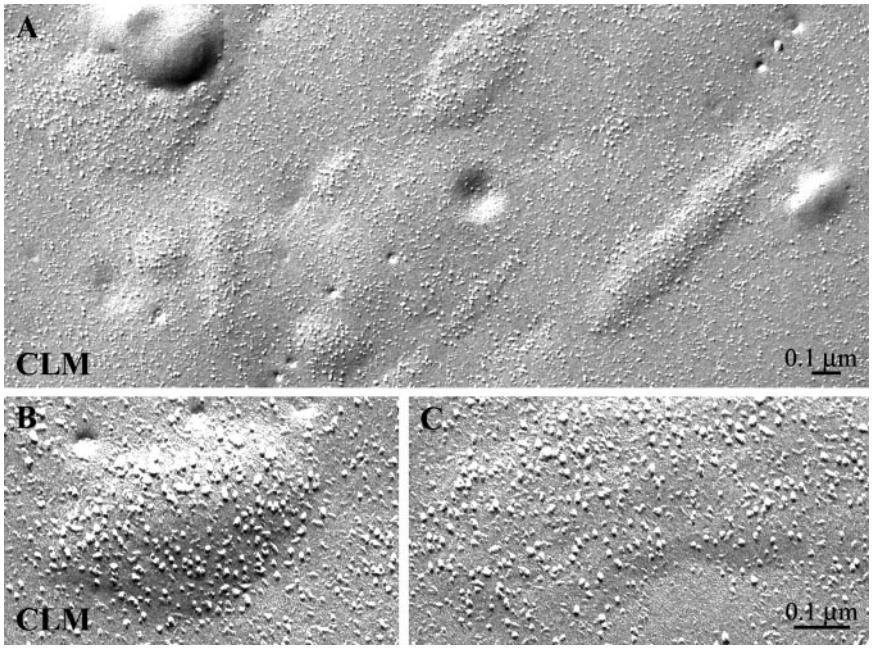

Figure 6. Replacing the II-III loop of α_{1C} with that of the *Musca* α_1 subunit does not restore tetrad formation. Freeze-fracture electron micrographs of chimera CLM, a cardiac DHPR with the *Musca* II-III loop sequence, expressed in dysgenic myotubes shows cardiac characteristics (A–C). Clusters of DHPRs (identifiable on basis of their large size) are visible within domed regions of the plasmalemma. Within the clusters, the particle density is fairly high, but the particles show no tendency toward a tetradic grouping (compare with Figures 3, E–F, and 4E for similar failure to restore tetrads by α_{1C} and SkLC).

However, e-c coupling properties and tetrad formation did no longer go hand in hand in a chimera in which the entire II-III loop has been replaced for the highly heterologous *Musca* II-III loop (chimera SkLM). Surprisingly this chimera still showed a fairly high degree of tetrad formation, even though it does not support e-c coupling (Wilkens *et al.*, 2001; Kugler *et al.*, 2004a). This might suggest that the *Musca* loop also contains the sequence information necessary for tetrad formation. However, the finding that the *Musca* II-III loop did not restore tetrad formation in the cardiac channel backbone (chimera CLM) does not support this idea. Alternatively, regions of the skeletal α_{1S} outside the II-III loop may contribute sufficiently to DHPR–RyR1 interactions to achieve some degree of tetrad formation with SkLM. Moreover, considering the low homology between α_{1S} and the *Musca* II-III loop (75% dissimilarity), it is rather unlikely that these two isoforms would share such an important interaction motif, whereas the highly homologous α_{1C} would not. The highest degree of homology between the α_{1S} and *Musca* II-III loop exists at the beginning and at the end of the loop, but most of these conserved residues also are found in the corresponding positions of the cardiac sequence, which did not support tetrad formation. Finally, an essential function in tetrad formation of these conserved residues near both ends of the II-III loop can be excluded based on the results from chimeras SkLC and $SkLCS_{46}$. These two chimeras clearly demonstrate that the critical determinants for tetrad formation reside exactly in the 46-amino acid sequence that is also the critical determinant for skeletal-type e-c coupling. Thus, our data indicate both an important role in tetrad formation of this specific 46-amino acid sequence in the II-III loop and the contribution of additional parts of the α_1 subunit outside the II-III loop.

Functional analysis of DHPR–RyR interactions cannot unequivocally identify the critical regions involved in the cross talk between the two molecules, unless the structure of the complex also is taken into consideration. Thus, although it is clear that substitution of the S46 region with cardiac and/or *Musca* sequences results in lack of e-c coupling (Nakai *et al.*, 1998; Grabner *et al.*, 1999; Wilkens *et al.*, 2001), the question remains whether this is simply due to a lack of proximity between the two molecules, as indicated by the absence of tetrads, rather than to a lack of the major functionally interactive domain. Our structural data with the SkLM and $SkLMS_{45}$ chimeras are illuminating. Both constructs form tetrads and thus place the DHPR in a position that would allow interaction to occur. However, only $SkLMS_{45}$ supports skeletal e-c coupling, indicating that the S45 region is indeed a major site for the functional interaction, as well as part of the mechanical link. Note that the reverse, which is skeletal e-c coupling in the absence of tetrads, was never observed.

The question remains how the postulated additional interaction sites can be sufficient for tetrad formation in SkLM and not in chimera SkLC, which has higher sequence homology to the skeletal DHPR? The most plausible explanation for this discrepancy would be a dominant negative effect of the cardiac II-III loop region corresponding to skeletal sequence 720–765. It is possible that this cardiac II-III loop sequence not only lacks the positive RyR1 interaction domain present in α_{1S} but also specifically interferes with the interactions that are responsible for the coordinated arrangement of the α_{1S} subunit and the RyR1. The model in Figure 7 suggests how multiple positive interaction domains in the skeletal sequence and an inhibitory signal in the cardiac II-III loop may lead to the observed behavior in the different α_1 subunits and chimeras analyzed in this study. In α_{1S}, multiple interaction domains cooperate in tetrad formation. In contrast, the cardiac II-III loop contains an inhibitory sequence, which may hinder tetrad formation not only in α_{1C} but also when placed into the skeletal background (SkLC) containing the additional interaction sites. The *Musca* II-III loop neither contains the positive skeletal nor the negative cardiac signal, and therefore when inserted into the skeletal channel (chimera SkLM) does not totally abolish tetrad formation via the additional skeletal interactions sites. The observation that the cardiac channel does not form tetrads even when the dominant negative effect of the II-III loop is replaced by the neutral *Musca* loop (CLM) suggests that the additional binding sites are specific to α_{1S} and are missing in α_{1C}. When the skeletal 45-amino acid sequence is

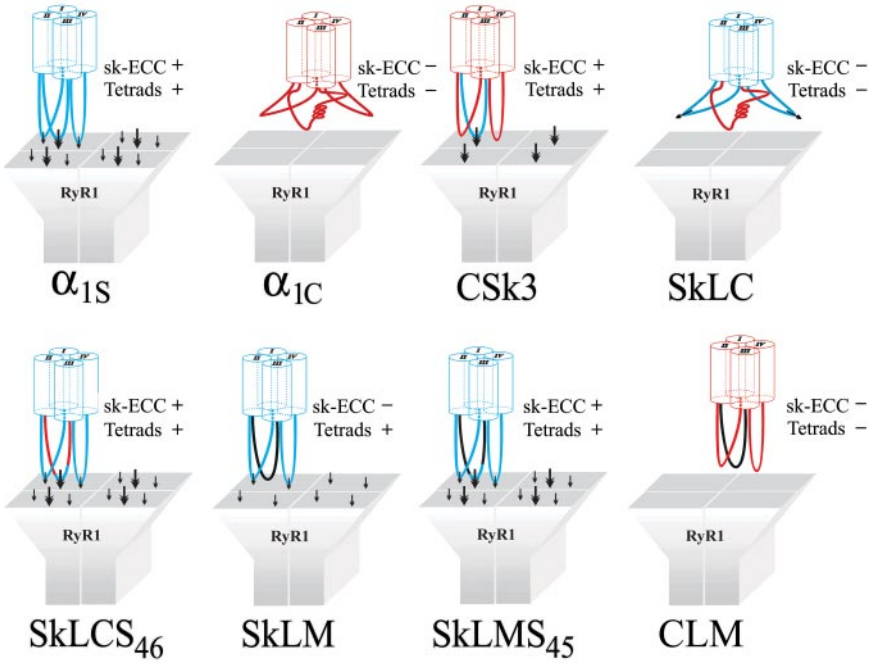

Figure 7. Model of DHPR–RyR1 interactions involved in tetrad formation. For each analyzed construct one of four DHPRs is shown opposite a RyR1, with the arrows indicating presumptive protein–protein interactions. Bold arrows represent the primary interaction sites in the DHPR II-III loop, and small arrows represent an unspecified number of additional α_{1S}-specific interaction sites; rabbit skeletal α_{1S} sequence is indicated in blue, cardiac α_{1C} sequence in red, and *Musca* α_1 sequence in black. In α_{1S} multiple interaction sites cooperate in tetrad formation. Whereas the skeletal II-III loop is sufficient to confer tetrad formation onto α_{1C} (CSk3), it is not absolutely necessary for tetrad formation as seen when it is replaced by the heterologous II-III loop of the *Musca* α_1 subunit (SkLM). However, the *Musca* II-III loop by itself is not able to coordinate α_{1C} into tetrads (CLM). The presence of a dominant inhibitory property in the cardiac II-III loop, probably a change in secondary structure, can explain the lack of tetrad formation in α_{1C} and in chimera SkLC. The restoration of tetrad formation in parallel with skeletal e-c coupling properties (sk-ECC) by transferring a 46-amino acid skeletal II-III loop sequence into the cardiac II-III loop of SkLC (resulting in chimera SkLCS$_{46}$) and the strengthening of tetrad formation in SkLMS$_{45}$ demonstrate that both the primary interaction site in the skeletal loop and the inhibitory signal in the cardiac loop reside within this short sequence, which also is the critical determinant for skeletal muscle e-c coupling.

added back into the *Musca* loop in the skeletal background (SkLMS$_{45}$), wild-type levels of tetrad formation are regained. Indeed, this chimera formed the most extensive and ordered arrays of tetrads, supporting a positive role for the S45 region in the actual linkage between DHPRs and RyRs.

So what is the nature of the positive and negative signals in the II-III loop? Tetrad formation by chimera SkLCS$_{46}$ indicates that the positive signal in α_{1S} as well as the negative signal in α_{1C} must be encoded within the corresponding 46-amino acid II-III loop sequences. If outside sequences or overall properties like the larger size of the cardiac II-III loop would inhibit the interaction with RyR1, tetrad formation should not be restored by replacing this sequence in the cardiac loop for that of α_{1S}. Recently, Kugler *et al.*, (2004a) reported a detailed characterization of the structural determinants of e-c coupling within the critical II-III loop sequence of the α_{1S} subunit. The minimal sequence necessary for skeletal e-c coupling contains a motif of four specific skeletal residues, which cannot be replaced by the corresponding cardiac residues without loss of e-c coupling properties. This motif may be a protein–protein binding site functioning in e-c coupling as well as in tetrad formation. In addition, the critical II-III loop sequence contains a conserved cluster of negatively charged amino acids, which has to form a random coil to support skeletal-type e-c coupling. In constructs in which this negatively charged amino acid cluster is predicted to form an α-helix, as for example in α_{1C} and SkLC, e-c coupling fails. It is possible that the α-helical conformation actively inhibits interactions between the α_1 subunit and the RyR1, in the simplest case by sterical hindrance, and thus blocks e-c coupling and tetrad formation. The *Musca* II-III loop does not contain either the putative binding motif or the cluster of negatively charged residues, nor is its secondary structure in this region predicted to be α-helical. This is consistent with the lack of skeletal muscle e-c coupling in SkLM and at the same time with its neutral property toward tetrad formation due to the absence of the putative inhibitory signal.

This novel view of the function of the II-III loop challenges existing concepts of the role of the II-III loop and has interesting implications on the mechanism of α_1 subunit–RyR1 interactions in general. The important question now is whether this mechanism applies only to tetrad formation or similarly to the role of the II-III loop in e-c coupling. Considering the existence of multiple interaction sites plus positive and negative effects of different II-III loops, skeletal DHPR–RyR interactions can no longer be reduced to a simple "plunger" function of the skeletal II-III loop. Rather, we shall view the tissue-specific contribution of the II-III loop as either facilitating (α_{1S}), inhibiting (α_{1C}), or as neutral (α_{1Musca}) to more complex DHPR–RyR1 interactions.

Several independent observations are consistent with the existence of additional interaction domains in α_{1S} outside the II-III loop that were not noted in studies based solely on α_{1S}/α_{1C} chimeras because they are conserved between the two channel isoforms. Work from the laboratory of R. Coronado (Beurg *et al.*, 1999) suggests a role of the calcium channel β_{1a} subunit in the communication between the α_{1S} and RyR1. Moreover, peptide-binding studies (Leong and MacLennan, 1998) implicate additional sequences in the III-IV loop in α_{1S}–RyR1 binding. Finally, the existence of a mutation in the III-IV loop of the human α_{1S} that leads to a malignant hyperthermia phenotype similar to numerous mutations in the RyR1 (Monnier *et al.*, 1997) suggests that this loop also may be involved in the interaction with the RyR1. Any or all of these putative interaction sites may represent the additional binding sites contributing to tetrad formation. However, the results with chimeras SkLM and SkLMS$_{45}$ show that although the additional interaction sites are sufficient for tetrad formation, they do not support skel-

etal muscle e-c coupling without the critical II-III loop sequence.

Protasi *et al*. (2002) and Nakai *et al*. (1998) have used coexpression of skeletal DHPR and skeletal/cardiac RyR chimeras to characterize the complementary sequences in the RyR1 that are responsible for the specific organization of the DHPR into tetrads and for their functional interaction with DHPRs. At least two domains within a large segment of the primary sequence (Sk 1635–3720) are involved in these interactions, and the results also show that tetrads are always present when skeletal e-c coupling is restored. Interestingly, however, among the multiple sequences involved, the ones that best restore e-c coupling are not identical with those that most effectively restore tetrads. In light of our present findings, it cannot be decided whether these RyR1 domains represent the specific interaction partners for the skeletal DHPR II-III loop or for the hitherto unspecified additional interaction domains.

Thus, our present finding that the II-III loop plays an important role in the tissue-specific organization of DHPRs in the triad, but that other domains are also important, and under certain experimental conditions, even sufficient for tetrad formation, is in line with evidence for multiple DHPR–RyR1 interaction sites. Nevertheless, the II-III loop determines the difference in the skeletal and cardiac properties. Our conclusion is that the mechanism by which it seems to accomplish this appears to be different from that previously envisioned, at least in terms of tetrad formation. So far, the focus was on the specific properties of the skeletal II-III loop. In the future, we may have to pay more attention to the specific properties of the cardiac II-III loop to understand how it functions to inhibit specific skeletal properties.

ACKNOWLEDGMENTS

This work was supported by National Institutes of Health grant AR P01144650 to C.F.A.; Grant-in-Aid for Scientific Research from the Japan Society for the Promotion of Science 14380019 and 14208005 to H.T; grant-in-aid for Scientific Research from the National Institute of Fitness and Sports, President's Discretionary Budget 2003 and 2004 to H.T.; grants of the Austrian Science Fund (Fond zur Förderung der wissenschofttichen Forschung) and the OeNB P16532-B05 to B.E.F and P13831-GEN and P16098-B11 to M.G.; and the European Commission's Improving Hurman Potential network grant HPRN-CT-2002-00331 to B.E.F.

REFERENCES

Ahern, C.A., Arikkath, J., Vallejo, P., Gurnett, C.A., Powers, P.A., Campbell, K.P., and Coronado, R. (2001). Intramembrane charge movements and excitation-contraction coupling expressed by two-domain fragments of the Ca^{2+} channel. Proc. Natl. Acad. Sci. USA *98*, 6935–6940.

Araque, A., Clarac, F., and Buno, W. (1994). P-type Ca^{2+} channels mediate excitatory and inhibitory synaptic transmitter release in crayfish muscle. Proc. Natl. Acad. Sci. USA *91*, 4224–4228.

Beurg, M., Ahern, C.A., Vallejo, P., Conklin, M.W., Powers, P.A., Gregg, R.G., and Coronado, R. (1999). Involvement of the carboxy-terminus region of the dihydropyridine receptor β1a subunit in excitation-contraction coupling of skeletal muscle. Biophys. J. *77*, 2953–2967.

Block, B.A., Imagawa, T., Campbell, K.P., and Franzini-Armstrong, C. (1988). Structural evidence for direct interaction between the molecular components of the transverse tubule/sarcoplasmic reticulum junction in skeletal muscle. J. Cell Biol. *107*, 2587–2600.

Cohen, S.A., and Pumplin, D.W. (1979). Clusters of intramembranous particles associated with binding sites for alpha-bungarotoxin in cultured chick myotubes. J. Cell Biol. *82*, 494–516.

Erxleben, C., and Rathmayer, W. (1997). A dihydropyridine-sensitive voltage-dependent calcium channel in the sarcolemmal membrane of crustacean muscle. J. Gen. Physiol. *109*, 313–326.

Flucher, B.E., Andrews, S.B., and Daniels, M.P. (1994). Molecular organization of t-tubule/SR junctions during development of excitation-contraction coupling in skeletal muscle. Mol. Biol. Cell *5*, 1105–1118.

Flucher, B.E., Kasielke, N., Gerster, U., Neuhuber, B., and Grabner, M. (2000b). Insertion of the full-length calcium channel α_{1S} subunit into triads of skeletal muscle in vitro. FEBS Lett. *474*, 93–98.

Flucher, B.E., Kasielke, N., and Grabner, M. (2000a). The triad targeting signal of the skeletal muscle calcium channel is localized in the COOH terminus of the α_{1S} subunit. J. Cell Biol. *151*, 467–477.

Flucher, B.E., Weiss, R.G., and Grabner, M. (2002). Cooperation of two-domain Ca^{2+} channel fragments in triad targeting and restoration of excitation-contraction coupling in skeletal muscle. Proc. Natl. Acad. Sci. USA *99*, 10167–10172.

Franzini-Armstrong, C. (1984). Freeze-fracture of frog slow-tonic fibers. Structure of surface and internal membrane. Tissue Cell *16*, 647–664.

Franzini-Armstrong, C., and Kish, J.W. (1995). Alternate disposition of tetrads in peripheral couplings of skeletal muscle. J. Muscle Res. Cell Motil. *16*, 319–324.

Giannini, G., Gonti, A., Mammarella, S., Scrobogna, M., and Sorrentino, V. (1995). The ryanodine receptor/calcium channel genes are widely and differentially expressed in murine brain and peripheral tissues. J. Cell Biol. *128*, 893–904.

Gilly, W.F., and Scheuer, T. (1994). Contractile activation in scorpion striated muscle fibres. J. Gen. Physiol. *81*, 321–345.

Grabner, M., Bachmann, A., Rosenthal, F., Striessnig, J., Schultz, C., Tautz, D., and Glossmann, H. (1994). Insect calcium channels. Molecular cloning of an α_1-subunit from housefly (*Musca domestica*) muscle. FEBS Lett. *339*, 189–194.

Grabner, M., Dirksen, R.T., and Beam, K.G. (1998). Tagging with green fluorescent protein reveals a distinct subcellular distribution of L-type and non-L-type Ca^{2+} channels expressed in dysgenic myotubes. Proc. Natl. Acad. Sci. USA *95*, 1903–1908.

Grabner, M., Dirksen, R.T., Suda, N., and Beam, K.G. (1999). The II-III loop of the skeletal muscle dihydropyridine receptor is responsible for the bi-directional coupling with the ryanodine receptor. J. Biol. Chem. *274*, 21913–21919.

Hencek, M., and Zachar, J. (1977). Calcium currents and conductances in the muscle membrane of the crayfish. J. Physiol. *476*, 315–322.

Jurman, M.E., Boland, L.M., Liu, Y., and Yellen, G. (1994). Visual identification of individual transfected cells for electrophysiology using antibody-coated beads. Biotechnology *17*, 876–881.

Kasielke, N., Obermair, G., Kugler, G., Grabner, M., and Flucher, B.E. (2003). Cardiac-type EC-coupling in dysgenic myotubes restored with Ca^{2+} channel subunit isoforms α_{1C} and α_{1D} does not correlate with current density. Biophys. J. *84*, 3816–3828.

Kugler, G., Weiss, R.G., Flucher, B.E., and Grabner, M. (2004a). Structural requirements of the dihydropyridine receptor α_{1S} II-III loop for skeletal-type excitation-contraction coupling. J. Biol. Chem. *279*, 4721–4728.

Kugler, G., Grabner, M., Platzer, J., Striessnig, J., and Flucher, B.E. (2004b). The monoclonal antibody mAb 1A binds to the excitation-contraction coupling domain in the II-III loop of the skeletal muscle calcium channel α_{1S} subunit. Arch. Biochem. Biophys. *427*, 91–100.

Leong, P., and MacLennan, D.H. (1998). The cytoplasmic loops between domains II and III and domains III and IV in the skeletal muscle dihydropyridine receptor bind to a contiguous site in the skeletal muscle ryanodine receptor. J. Biol. Chem. *273*, 29958–29964.

Mikami, A., Imoto, K., Tanabe, T., Niidome, T., Mori, Y., Takeshima, H., Narumiya, S., and Numa, S. (1989). Primary structure and functional expression of the cardiac dihydropyridine-sensitive calcium channel. Nature *340*, 230–233.

Monnier, N., Procaccio, V., Stieglitz, P., and Lunari, J. (1997). Malignant-hyperthermia susceptibility is associated with a mutation of the alpha1-subunit of the human dihydropyridine-sensitive L-type voltage-dependent calcium-channel receptor in skeletal muscle. Am. J. Hum. Genet. *60*, 1316–1325.

Nakai, J., Dirksen, R.T., Nguyen, H.T., Pessah, I.N., Beam, K.G., and Allen, P.D. (1996). Enhanced dihydropyridine receptor channel activity in the presence of ryanodine receptor. Nature *380*, 72–75.

Nakai, J., Tanabe, T., Konno, T., Adams, B., and Beam, K.G. (1998). Localization in the II-III loop of the dihydropyridine receptor of a sequence critical for excitation-contraction coupling. J. Biol. Chem. *273*, 24983–24986.

Osame, M., Engel, A.G., Rebouche, C.J., and Scott, R.E. (1981). Freeze-fracture electron microscopic analysis of plasma membranes of cultured muscle cells in Duchenne dystrophy. Neurology *31*, 972–979.

Powell, J.A., Petherbridge, L., and Flucher, B.E. (1996). Formation of triads without the dihydropyridine receptor alpha subunits in cell lines from dysgenic skeletal muscle. J. Cell Biol. *134*, 375–387.

Proenza, C., O'Brien, J.J., Nakai, J., Mukherjee, P.D., Allen, P.D., and Beam, K.G. (2002). Identification of a region of RyR1 that participates in allosteric coupling with the α_{1S} ($Ca_v1.1$) II-III loop. J. Biol. Chem. *277*, 6530–6535.

Protasi, F., Sun, X.H., and Franzini-Armstrong, C. (1996). Formation and maturation of the calcium release apparatus in developing and adult avian myocardium. Dev. Biol. *173*, 265–278.

Protasi, F., Franzini-Armstrong, C., and Allen, P.D. (1998). Role of the ryanodine receptors in the assembly by calcium release units in skeletal muscle. J. Cell Biol. *140*, 831–842.

Protasi, F., Franzini-Armstrong, C., and Flucher, B.E. (1997). Coordinated incorporation of skeletal muscle dihydropyridine receptors and ryanodine receptors in peripheral couplings of BC3H1 cells. J. Cell Biol. *137*, 859–870.

Protasi, F., Takekura, H., Wang, Y., Chen, S.R., Meissner, G., Allen, P.D., and Franzini-Armstrong, C. (2000). RyR1 and RyR3 have different roles in the assembly of calcium release units of skeletal muscle. Biophys. J. *79*, 2494–2508.

Protasi, F., Paolini, C., Nakai, J., Beam, K.G., Franzini-Armstrong, C., and Allen, P.D. (2002). Multiple regions of RyR1 mediate functional and structural interactions with α1S-dihydropyridine receptors in skeletal muscle. Biophys. J. *83*, 3230–3244.

Sun, X.H., Protasi, F., Takahashi, H., Takeshima, H., Ferguson, D.G., and Franzini-Armstrong, C. (1995). Molecular architecture of membranes involved in excitation-contraction coupling of cardiac muscle. J. Cell Biol. *129*, 659–671.

Takekura, H., Bennett, L., Tanabe, T., Beam, K.G., and Franzini-Armstrong, C. (1994). Restoration of junctional tetrads in dysgenic myotubes by dihydropyridine receptor cDNA. Biophys. J. *67*, 793–803.

Takekura, H., Nishi, M., Noda, T., Takeshima, H., and Franzini-Armstrong, C. (1995). Abnormal junctions between surface membrane and sarcoplasmic reticulum in skeletal muscle with a mutation targeted to the ryanodine receptor. Proc. Natl. Acad. Sci. USA *92*, 3381–3385.

Takekura, H., and Franzini-Armstrong, C. (2002). The structure of Ca^{2+} release units in arthropod body muscle indicates an indirect mechanism for excitation-contraction coupling. Biophys. J. *83*, 2742–2753.

Tanabe, T., Beam, K.G., Adams, B.A., Niidome, T., and Numa, S. (1990). Regions of the skeletal muscle dihydropyridine receptor critical for excitation-contraction coupling. Nature *346*, 567–569.

Tanabe, T., Takeshima, H., Mikami, A., Flockerzi, V., Takahashi, H., Kangawa, K., Kojima, M., Matsuo, H., Hirose, T., and Numa, S. (1987). Primary structure of the receptor for calcium channel blockers from skeletal muscle. Nature *328*, 313–318.

Wilkens, C.M., Kasielke, N., Flucher, B.E., Beam, K.G., and Grabner, M. (2001). Excitation-contraction coupling is unaffected by drastic alteration of the sequence surrounding residues L720–L764 of the α_{1S} II-III loop. Proc. Natl. Acad. Sci. USA *98*, 5892–5897.